

Synthesis and Characterization of Cadmium-Thioacetamide Nanocomposites Using a Facile Sonochemical Approach: A precursor for Producing CdS Nanoparticles via Thermal Decomposition

Maryam Ranjbar^{1*}, Mostafa Yousefi¹, Robabeh Nozari², Shabnam Sheshmani²

1- Department of Chemical Technologies, Iranian Research Organization for Science and Technology (IROST), Tehran, I. R. Iran

2- Department of Chemistry, Faculty of Sciences, Islamic Azad University, Shahr-e-Rey Branch, Tehran, I. R. Iran

(* Corresponding author: marandjbar@irost.ir

(Received: 25 Aug. 2013 and Accepted: 19 Nov. 2013)

Abstract:

In this investigation, we report facile synthesis of cadmium(II)-thioacetamide nanocomposites in the presence and absence of polyvinyl alcohol under ultrasonic irradiations, using cadmium acetate dihydrate ($\text{Cd}(\text{CH}_3\text{COO})_2 \cdot 2\text{H}_2\text{O}$), potassium iodide (KI), thioacetamide (TAA, CH_3CSNH_2), and polyvinyl alcohol (PVA) as the starting materials. Results show that in the presence of polyvinyl alcohol sizes of the particles reduce. Characterization of the compounds was carried out by determination of melting point, scanning electron microscopy (SEM), energy dispersive X-ray analysis (EDAX), Fourier transform infrared (FT-IR) spectroscopy, $^1\text{H-NMR}$ spectroscopy and thermogravimetric-differential thermal analyses (TG/DTA). The thermal decomposition of the polymeric nanocomposite, Cd-thioacetamide/PVA in an autoclave under critical condition led to the formation of spherical cadmium sulfide nanoparticles with an average particle size of about 20 nm. The X-ray diffraction pattern at room temperature revealed that highly pure and crystallized CdS with hexagonal structure were obtained. The sonochemical method resulted in a significant reduction of reaction time, reaction temperature and particle size of the products.

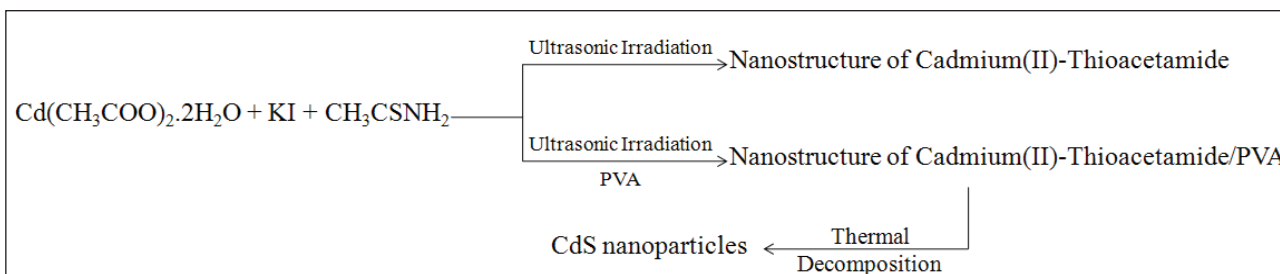
Keywords: Nanocomposite, Sonochemical method, Thioacetamide, Cadmium sulfide nanoparticles.

1. INTRODUCTION

In recent years, the synthesis of inorganic materials with specific size and morphology has attracted considerable attention. Their excellent physical and chemical properties in various fields, such as catalysis, sensors, solar cells, photo detectors, light emitting diodes and laser communication, have made them very attractive and promising materials [1-4]. It is well documented that materials with

nano-scale grain size show different properties relative to the same material in bulk form [5-7].

In order to synthesis various nano-materials many different synthetic approaches like chemical vapor deposition (CVD), thermal evaporation, chemical bath deposition, laser ablation, hydrothermal, homogeneous precipitation in an organic matrix, sonochemical and sol-gel method have been utilized [8-15]. Sonochemistry is the research area in which molecules undergo a chemical reaction due



Scheme 1: Materials produced and synthetic methods.

to the application of powerful ultrasound radiation [16, 17]. The efficiency of heterogeneous reactions involving solids dispersed in liquids depends upon the available reactive surface area and mass transfer. The ultrasonically-enhanced mass transport is thought to be due to two transient processes: (1) Bubble collapse at or near the solid–liquid interface with microjet directed towards the surface, and (2) Bubble motion near or within the diffusion layer of the surface.

From an inorganic chemistry point of view, most of the effects of interest regarding ultrasonication are related to cavitation. Cavitation causes solute thermolysis along with the formation of highly reactive radicals and molecules [18]. In addition, if a solid is presented in solution, the sample size of the particles is diminished by solid disruption, thereby increasing the total solid surface in contact with the solvent [19]. The use of high-intensity ultrasound to enhance the reactivity of metals as a stoichiometric reagent has become a synthetic technique for many heterogeneous organic and organometallic reactions [20-23]. It is well known that control of the size, morphology and structure represents some of key issues in nanotechnology that determine their properties.

Semiconductor materials with nano dimensions have attracted a lot of attention in recent years due to their potential applications in diverse electronic nanodevices [24–26]. Among binary compound semiconductors, cadmium sulfide (CdS) is representative of group II due to its wideband gap of 2.42 eV at room temperature, which is widely used in solar cells [27], light emitting diodes [28], photocatalysts, lasers [29], biological imaging and labeling applications [30]. There are

many experimental approaches to synthesize CdS nanoparticles such as microwave-solvothermal synthesis [31, 32], hydrothermal method [33, 34] and surfactant-ligand co-assisting solvothermal method [35]. Most of the products have different morphologies such as dendrites [36], flakes [37], spheres [38], nanorods [39, 40], nanowires [41-43], triangular and hexagonal plates [44], flower-like shape [45] and sea-urchin-like shape [46].

In the present work, we report the synthesis of Cd(II)-thioacetamide nanocomposites in the presence and absence of polyvinyl alcohol under ultrasonic irradiations, employing cadmium acetate dihydrate ($\text{Cd}(\text{CH}_3\text{COO})_2 \cdot 2\text{H}_2\text{O}$), potassium iodide (KI), thioacetamide (TAA, CH_3CSNH_2), and polyvinyl alcohol (PVA, $M_w \cong 100,000$; hydrolysis degree=98%-99%) as the starting materials. We also describe the preparation of CdS nanoparticles with hexagonal morphology by thermal decomposition of the polymeric nanocomposite, Cd-thioacetamide/PVA as precursor. We choose thioacetamide as the S^{2-} source. It is easier for thioacetamide to release S^{2-} ions. We introduce polyvinyl alcohol (PVA) as protecting materials to the morphology-controlled synthesis of CdS nanoparticles.

2. EXPERIMENTAL

2.1. Materials and physical measurements

The raw materials used in this work were of purities above 99%, therefore no further purification was required. All solutions were prepared with double distilled deionized water. A multiwave ultrasonic generator (UP400S, Hielscher), equipped with a converter/transducer and titanium oscillator (horn),

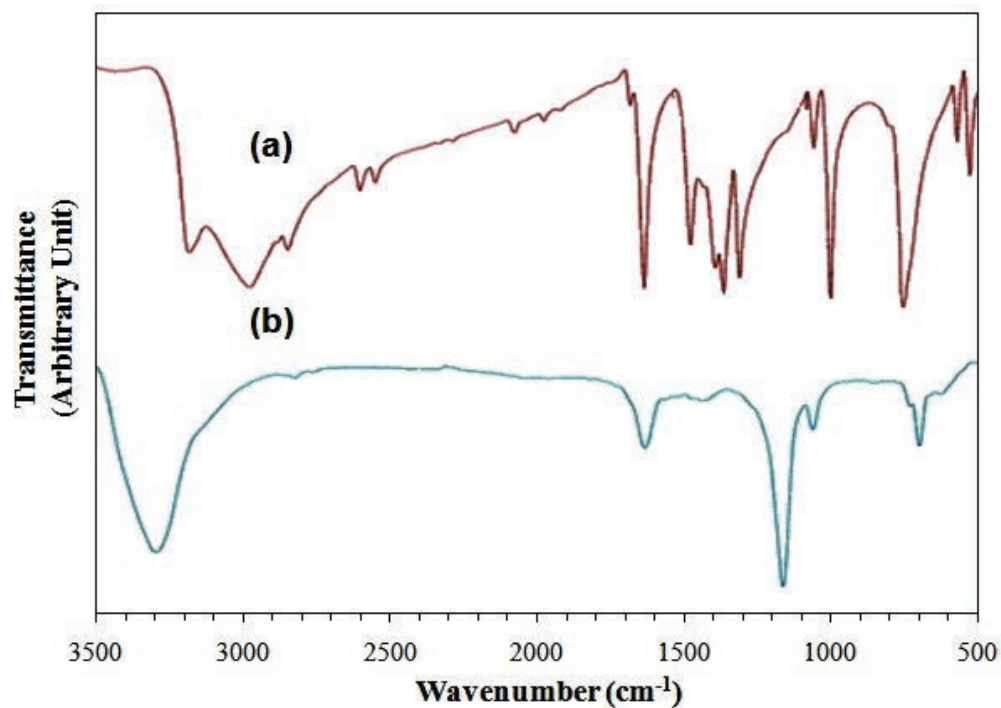


Figure 1: FT-IR spectra of (a) thioacetamide and (b) Cd-thioacetamide nanocomposite.

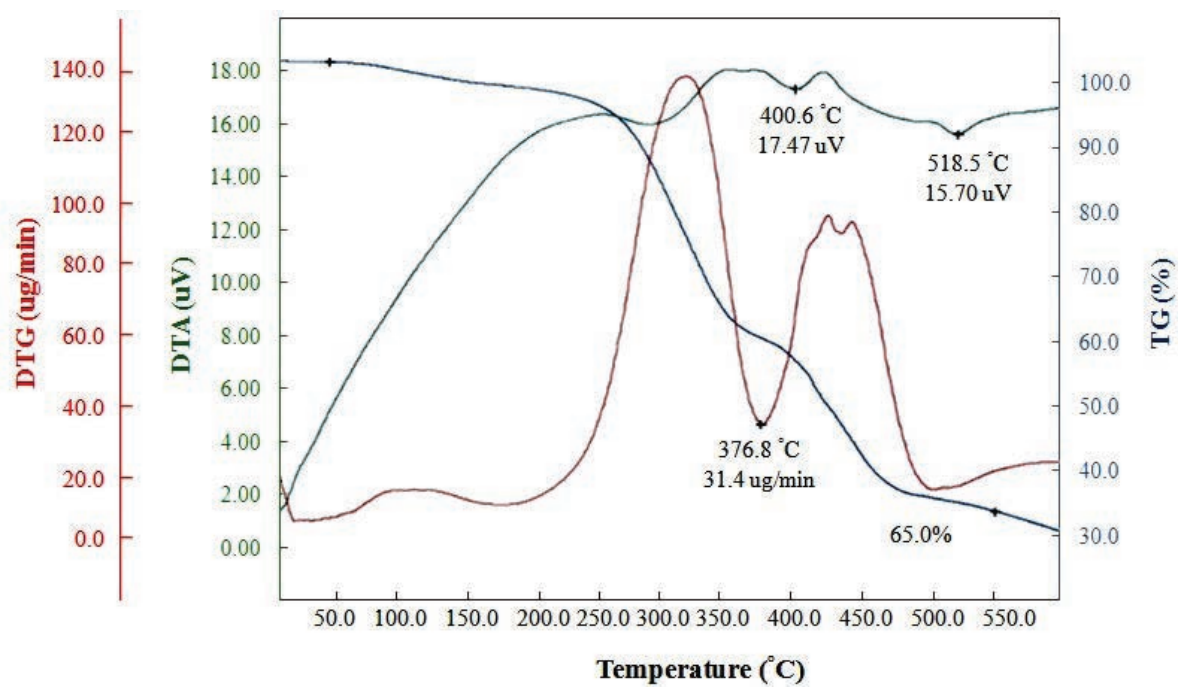


Figure 2: TG/DTA curves of Cd-thioacetamide nanocomposite.

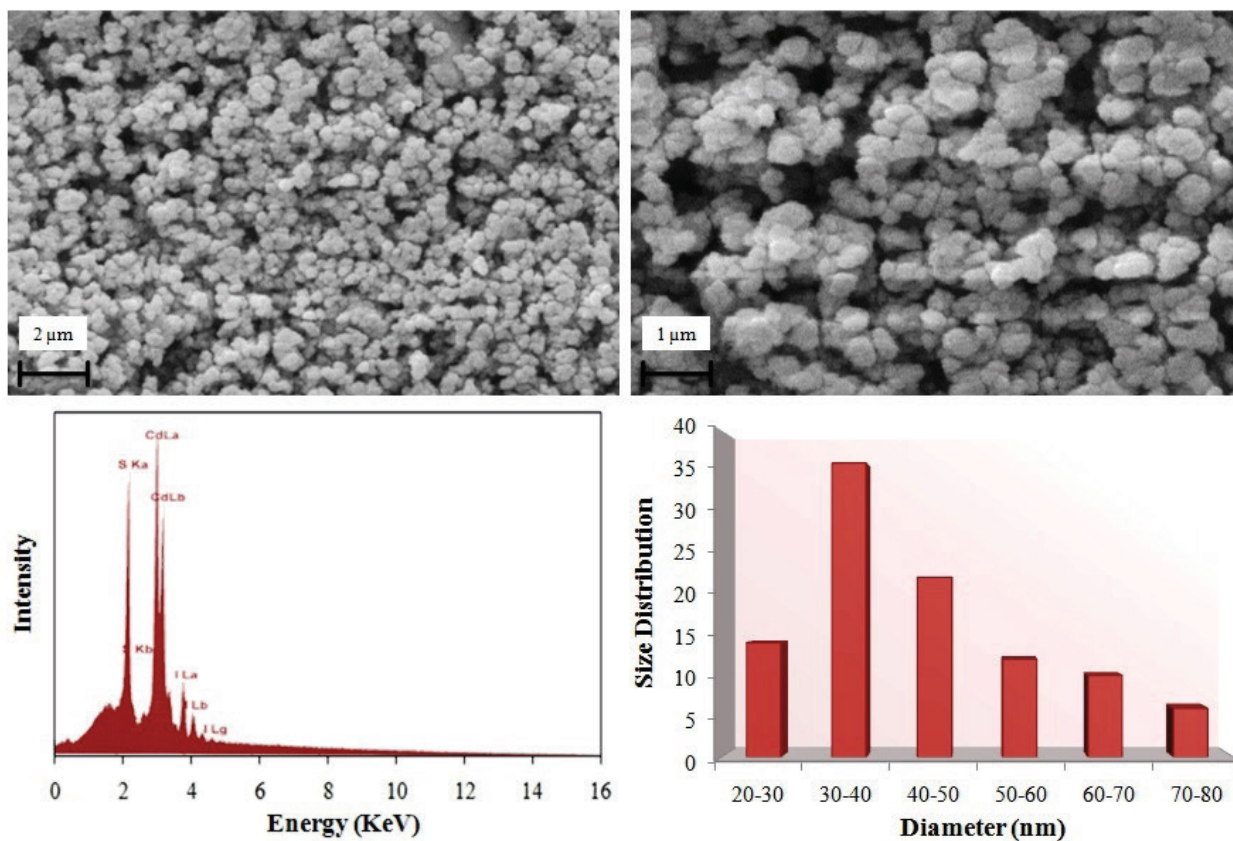


Figure 3: (a, b) SEM images, (c) EDAX spectrum, and (d) the corresponding particle size distribution histogram of Cd-thioacetamide nanocomposite.

12.5 mm in diameter, operating at 24 kHz with 8% power output of 400 W, was used for ultrasonic irradiation. The ultrasonic generator automatically adjusts the power level.

Melting points (uncorrected) were measured with a Branstead Electrothermal 9100 apparatus. Fourier transform infrared (FT-IR) spectra were recorded using Bruker tensor 27 spectrophotometer in a KBr matrix. X-ray powder diffraction (XRD) measurements were performed using an X'pert diffractometer of Philips Company with graphite monochromatic Cu K α ($\lambda = 0.15418$ nm) radiation at room temperature in the 2θ range of 10-60°. The samples were characterized by using scanning electron microscopy (SEM) and energy dispersive X-ray (EDX) techniques (Philips XL30) with gold coating.

Thermogravimetric and differential thermal analyses (TGA/DTA) were carried out with Pyris Diamond

Perkin Elmer under air atmosphere at a heating rate of 10 °C/min from room temperature to 600 °C. Nuclear magnetic resonance ($^1\text{H-NMR}$) spectrum of precursor was recorded by Bruker (400 MHz) in DMSO- d_6 . Gel permeation chromatograms were measured on a Waters GPC system consisting of an isocratic pump, solvent degasser, column oven, 2996 photo diode array (PDA) detector, 2414, refractive index detector, 717 plus auto sampler and a Styragel HT 4 GPC column with precolumn installed. Linear PMMA standards were used for calibration. The solvent was DMF containing 5 mmol/L NH_4PF_6 . The flow speed was 0.5 mL/min.

2.2. Preparation of Cd(II)-thioacetamide nanocomposites by sonochemical process

In a typical synthesis procedure, 0.532 g of cadmium (II) acetate dihydrate, 0.148 g of thioacetamide and 0.664 g of potassium iodide were dissolved in 20

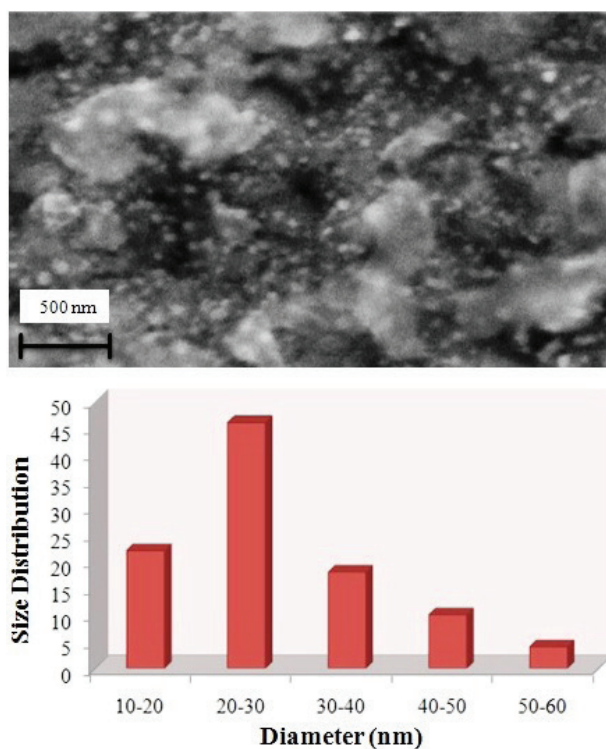


Figure 4: (a) SEM image, and (b) the corresponding particle size distribution histogram of polymeric Cd-thioacetamide/PVA nanocomposite.

mL double distilled deionized water. This solution was irradiated with a high intensity ultrasonic horn (24 kHz, 400W) at room temperature for 1 h. During the sonication of the reaction mixture the temperature increased to 70-80°C as measured by an iron-constantin thermocouple. After one hour a bright yellow precipitate formed. It was isolated by centrifugation (4,000 rpm, 15 min), washed with double distilled water and then with absolute ethanol in order to remove residual impurities and finally dried in air (yield: 0.915 g, 68%). Dec. p.200°C. To prepare of polymeric nanocomposite, 1.992 g of polyvinyl alcohol was dissolved in 20 mL of double distilled deionized water and then added into the above solution. This mixture was irradiated with ultrasonic waves for 1 h when a bright orange product formed.

2.3. Preparation of CdS nanoparticles

To obtain of CdS nanoparticles, 0.29 g of polymeric nanocomposite, Cd-thioacetamide/PVA and 20 mL double distilled deionized water was transferred into a Teflon-lined stainless autoclave (50 mL capacity). The autoclave was sealed and maintained at 200 °C for 30 h. The system was then cooled to ambient temperature naturally. The final product

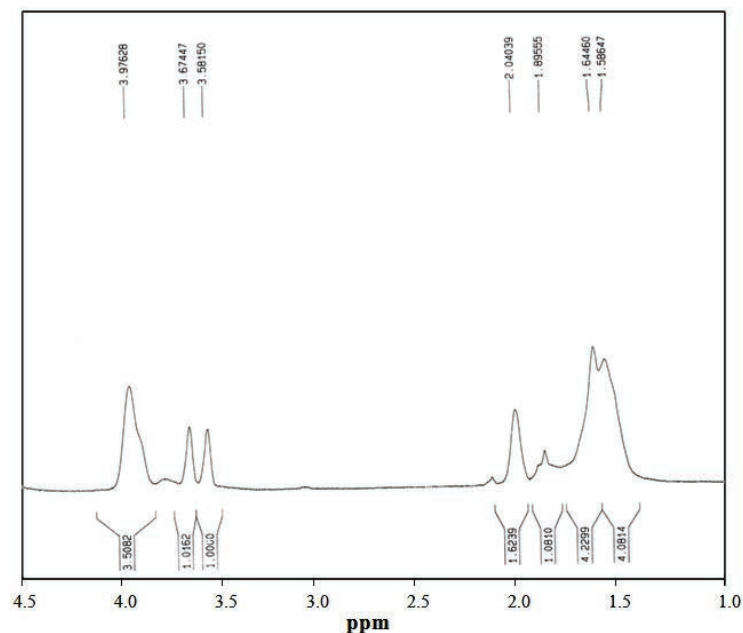


Figure 5: ¹H-NMR spectrum of polymeric Cd-thioacetamide/PVA nanocomposite.

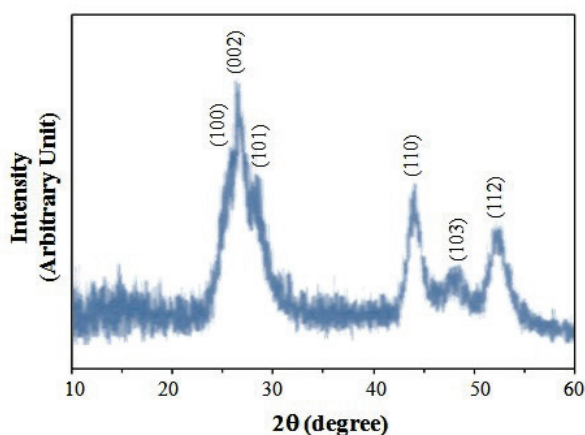


Figure 6: XRD pattern of CdS nanoparticles prepared by thermal decomposition of polymeric Cd-thioacetamide/PVA nanocomposite.

was collected and washed with distilled water and absolute ethanol several times, dried in air, and kept for further characterization.

3. RESULTS AND DISCUSSION

Reaction between thioacetamide ligand with a mixture of cadmium(II) acetate dihydrate and potassium iodide in the presence and absence of polyvinyl alcohol under ultrasonic irradiations, led to the formation of Cd(II)-thioacetamide nanocomposites. Scheme 1 gives an overview of the method used for the synthesis of cadmium(II) containing nanostructures.

Thioacetamide is an organic sulfur compound that has lone pair electrons on nitrogen and sulfur atoms, and is able to donate lone pair electrons to form coordination compound with the vacant d-orbital of Cd cations. The first step to check the purity of the Cd(II) nanocomposites was a melting point measurement, which was quite different from starting materials indicating a new product formation. FT-IR spectra of thioacetamide and Cd-thioacetamide nanocomposite in the frequency range from 3,500 to 500 cm^{-1} , are compared in Figure 1. By comparing the FT-IR spectrum of thioacetamide (Figure 1a) and the FT-IR spectrum of Cd-thioacetamide nanocomposite (Figure 1b), it was found that thioacetamide ligand was

coordinated to Cd^{2+} ion, and the Cd-thioacetamide nanocomposite formed.

The N-H stretching vibrations shifted from 3298 and 3080 cm^{-1} of thioacetamide to 3434 cm^{-1} of Cd-thioacetamide nanocomposite, while the peak at 3080 cm^{-1} corresponding to the N-H bond disappeared. The C-N stretching vibrations shifted from 1691 and 1479 cm^{-1} of thioacetamide to 1631 cm^{-1} of Cd-thioacetamide nanocomposite, and C=S stretching vibrations shifted from 973 and 712 cm^{-1} of thioacetamide to 1120 cm^{-1} and 619 cm^{-1} of Cd-thioacetamide nanocomposite. The change in bonding energy of N-H revealed the coordination of cadmium ions and thioacetamide molecules.

It can be concluded that nitrogen atoms of thioacetamide molecules were used to form Cd-thioacetamide nanocomposite, caused by donating lone pair electrons on nitrogen atoms, to form coordination compound with the vacant d-orbital of Cd cations.

To examine the thermal stability of Cd-thioacetamide nanocomposite, thermogravimetric and differential thermal analyses (TG/DTA) were carried out between 30 and 600°C in air (Figure 2). Complex was stable up to 70°C due to the water molecule began to be removed and decomposition took place between 70 and 550°C with a mass loss of 65%. As shown in Figure 2, three weight loss steps are shown in the TG curve. According to the TG curve, the weight loss 376°C up to 550°C is corresponding to the removal of thioacetamide ligand. Decomposition of the nanocomposite occurs to ultimately give solid that appears to be CdS. Mass loss calculations of the end residue and the XRD pattern of the final decomposition product (Figure 6) indicated the formation of CdS. The DTA curve displays three distinct endothermic peaks at 320°C, 400°C, and 518°C (Figure 2).

The morphology and size of Cd-thioacetamide and Cd-thioacetamide/PVA nanocomposites prepared by the sonochemical method were characterized by scanning electron microscopy (SEM) which showed composition of particles with sizes of about 38 nm and 25 nm, respectively. Figure 3a, 3b and 3d show the scanning electron microscopy (SEM) and the corresponding particle size distribution histograms of the Cd-thioacetamide

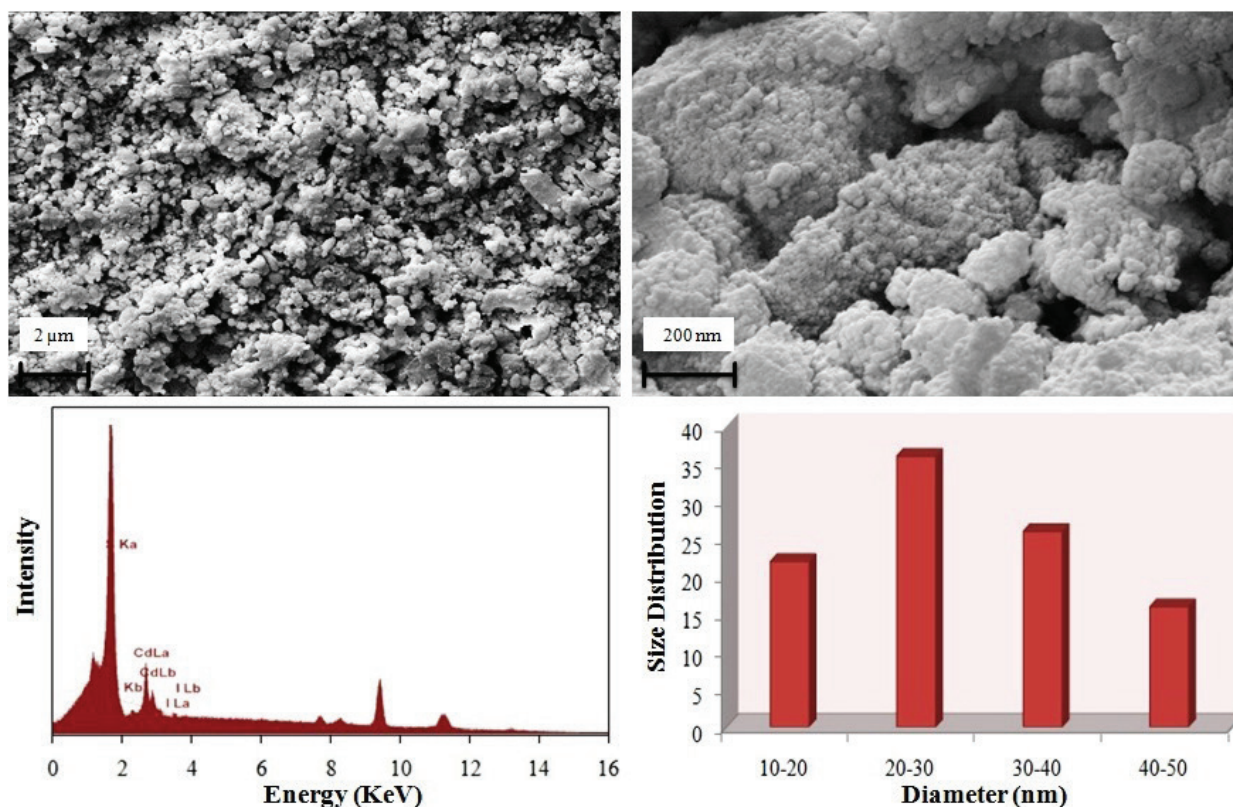


Figure 7: (a, b) SEM images, (c) EDAX spectrum, and (d) the corresponding particle size distribution histogram of CdS nanoparticles.

nanocomposite, respectively. This micrograph reveals that nanostructure of Cd-thioacetamide nanocomposite is uniform in shape and size. Also, spherical shaped morphology has been observed for the nanoparticles.

Figure 4 shows the scanning electron microscopy (SEM) and the corresponding particle size distribution histograms of the polymeric Cd-thioacetamide/PVA nanocomposite and as a result, the nanoparticles aggregate randomly to form almost uniform shape. The energy dispersive X-ray analysis (EDAX) of the Cd-thioacetamide nanocomposite, confirmed the presence of cadmium, sulfur, and iodide atoms as the elementary components (Figure 3c). By comparing SEM images of Cd(II)-thioacetamide nanocomposites, it was found that in presence of PVA the particles diameter decreased from about 38 nm to 25 nm which can be caused by spatial

exclusion of polymer molecules of polyvinyl alcohol, which provides a uniform environment.

To further study of Cd-thioacetamide/PVA nanocomposite, $^1\text{H-NMR}$ (400 MHz) spectrum was recorded. Figure 5 shows the $^1\text{H-NMR}$ spectrum of polymeric Cd-thioacetamide/PVA nanocomposite. Regardless of the solvent peaks at the chemical shifts of 3.5-3.6 ppm, the peaks appeared at the chemical shifts of 1.5-1.8 ppm could be assigned to the protons of methyl group in thioacetamide and the protons of CH_2 in PVA. Also, the peak appeared at the chemical shifts of 2 ppm, and the peak appeared at 3.9 ppm could be assigned to the proton of CH attached to hydroxyl group in PVA, and the protons of amide group in thioacetamide, respectively.

Figure 6 shows the representative XRD pattern of the CdS synthesized by hydrothermal route. It is obvious that all the diffraction peaks can be indexed to hexagonal phase CdS with P63mc space

group and lattice parameters of $a=4.1409 \text{ \AA}$ and $c=6.7198 \text{ \AA}$ (JCPDS file No.41-1049). Compared with the standard diffraction pattern, no peaks of impurities were detected, indicating the high purity of the product. In addition, the intense and sharp diffraction peaks suggest the obtained product is well crystallized. The broadness of the peaks indicates the small dimensions of the produced CdS nanoparticles. Estimated from the Scherer formula, $D=0.89\lambda/\beta\cos\theta$, where D is the average grain size, λ is the X-ray wavelength (0.15418 nm) and θ and β are the diffraction angle and full-width at half maximum of an observed peak, respectively [47], upon the main peak, the average size of the particles of sample was calculated to be 22 nm which is in agreement with that observed from the SEM image. The morphology of the CdS nanoparticles was characterized by scanning electron microscopy (SEM) and shows that it is composed of particles with sizes of about 20 nm. Figure 7a, 7b and 7d show the SEM images and the corresponding particle size distribution histogram of the CdS nanoparticles, respectively.

As it can be seen, a uniform nanometer scale particles with good size distribution is observed for the nanoparticles. To further confirm the chemical composition of the as-prepared CdS, EDAX spectrum was recorded. The very strong peaks related to Cd and S were found in the spectrum (Figure 7c) and no impurity was detected.

4. CONCLUSION

In summary, we prepared cadmium(II)-thioacetamide nanocomposites in the presence and absence of polyvinyl alcohol by sonochemical method. The SEM results demonstrated that in presence of PVA the sizes of the particles decreased from about 38 nm to 25 nm. Then we synthesized hexagonal CdS nanoparticles with spherical morphology from thermal decomposition of the polymeric nanocomposite, cadmium(II)-thioacetamide/PVA as precursor. The size of the CdS nanoparticles was measured both by XRD and SEM and the results were in very good agreement with each other.

The polymeric Cd(II) nanocomposite was a suitable

precursor for preparation of cadmium sulfide nanoparticles with interesting morphologies. All results revealed that ultrasonic synthesis can be employed successfully as a simple, efficient, low cost, environmentally friendly and very promising method for the synthesis of nanoscale materials without a need for special conditions, such as high temperature, long reaction times, and high pressure. This method may be extending to synthesize other metal sulfide nanocrystallites, nanowires, nanodisks, and even nanotubes.

ACKNOWLEDGMENTS

The authors would like to express gratitude for support by Nanotechnology Initiative Council, Iranian Research Organization for Science and Technology (IROST), and Islamic Azad University, Shahr-e-Ray branch.

REFERENCES

1. V. P. Singh, R.S. Singh, G. W. Thompson, V. Jayaraman, S. Sanagapalli, V. K. Rangari, *Sol. Energy Mater. Sol. Cells*, Vol. 81, (2004), p. 293.
2. G. H. Shahverdizadeh, A. Morsali, *J. Inorg. Organomet. Polym.*, Vol. 21, (2011), p. 694.
3. M. Payehghadr, V. Safarifard, M. Ramazani, A. Morsali, *J. Inorg. Organomet. Polym.*, Vol. 22, (2012), p. 543.
4. L. Hashemi, M. Hosseinfard, V. Amani, A. Morsali, *J. Inorg. Organomet. Polym.* doi: 10.1007/s10904-012-9786-5 (2012).
5. G. Marban, A. Lopez, I. Lopez, T. Valdes-Solis, *Appl. Catal. B Env.*, Vol. 99, (2010), p. 257.
6. T. Valdes-Solis, G. Marban, A.B. Fuertes, *Catal. Today*, Vol. 116, (2006), p. 354.
7. S. D. Jones, L.M. Neal, M.L. Everett, G.B. Hoflund, E.H.H. Weaver, *Appl. Sur. Sci.*, Vol. 256, (2010), p. 7345.
8. Y. Wu, P. Yang, *Chem. Mater.*, Vol. 12, (2000), p. 605.
9. S. Iijima, *Nature*, Vol. 354, (1991), p. 56.
10. A. M. Morales, C. M. Lieber, *Science*, Vol. 279,

- (1998), p. 208.
11. C. Suci, L. Gagea, A.C. Hoffmann, M. Mocean, Chem. Eng. Sci., Vol. 61, (2006), p. 7831.
 12. M. Salavati-Niasari, G. Hosseinzadeh, F. Davar, J. Alloys Compd., Vol. 509, (2011), p.134.
 13. M. Ranjbar, Ö. Çelik, S.H. Mahmoudi Najafi, S. Sheshmani, N. Akbari Mobarakeh, J. Inorg. Organomet. Polym., Vol. 22, (2012), p. 837.
 14. M. Ranjbar, E. Malakooti, S. Sheshmani, J. doi., Vol. 115, No. 10, (2013), p. 560983.
 15. M. Khorasani-Motlagh, M. Noroozifar, A. Ahanin-Jan, J. Iran. Chem., Soc., Vol. 9, (2012), p. 833.
 16. K.S. Suslick, Science, Vol. 247, (1990), p.1 439.
 17. K. H. Kim, K.B. Kim, Ultrason. Sonochem., Vol. 15, (2008), p. 1019.
 18. G. Wibetoe, D.T. Takuwa, W. Lund, G. Sawula, J. Anal. Chem., Vol. 363, (1999), p. 46.
 19. J. L. Capelo-Martínez, P. Ximénez-Embún, Y. Madrid, C. Cámara, Trends Anal. Chem., Vol. 23, (2004), p. 331.
 20. M.Y. Masoomi, A. Morsali, RSC Advances, Vol. 3, (2013), p. 19191.
 21. A. Morsali, M.Y. Masoomi, Coord. Chem. Rev., Vol. 253, (2009), p. 1882.
 22. M.Y. Masoomi, A. Morsali, Coord. Chem. Rev., Vol. 256, (2012), p. 2921.
 23. M.Y. Masoomi, G. Mahmoudi, A. Morsali, J. Coord. Chem., Vol. 63, (2010), p. 1186.
 24. B.I. Ipe, C. M. Niemeyer, Angew. Chem. Int. Ed., Vol. 45, (2006), p. 504.
 25. Y. Yang, O. Chen, A. Angerhofer, Y.C. Cao, J. Am. Chem. Soc., Vol. 128, (2006), p. 12428.
 26. D. Yu, J. Wu, Q. Gu, H. Park, J. Am. Chem. Soc., Vol. 128, (2006), p. 8148.
 27. T. Thongtem, C. Pilapong, S. Thongtem, Curr. Appl. Phys. Vol. 9, (2009), p. 1272.
 28. W. T. Yao, S.H. Yu, S.J. Liu, J.P. Chen, X.M. Liu, F.Q. Li, J. Phys. Chem., B., Vol. 110, (2006), p. 11704.
 29. S. Ghosh, A. Mukherjee, H. Kim, C. Lee, Mater. Chem. Phys., Vol. 78, (2003), p. 726.
 30. Z. Jun, D. Xiao-wei, L. Zhi-liang, X. Gang, X. Sheng-ming, Z. Xing-ping, Trans. Nonferrous Met. Soc. China, Vol. 17, (2007) 1367.
 31. A.V. Murugan, R.S. Sonawane, B.B. Kale, S.K. Apte, A.V. Kulkarni, Mater. Chem. Phys., Vol. 71, (2001), p. 98.
 32. S.-H. Yu, J. Yang, Z.-H. Han, Y. Zhou, R.-Y. Yang, Y.-T. Qian, Y.-H. Zhanga, J. Mater. Chem., Vol. 9, (1999), p. 1283.
 33. C. Li, X. Yang, B. Yang, Y. Yan, Y.T. Qian, J. Cryst. Growth, Vol. 291, (2006), p. 45.
 34. J. Yang, J.H. Zeng, S.H. Yu, L. Yang, G.E. Zhou, Y.T. Qian, Chem. Mater. Vol. 12, (2000), p. 3259.
 35. C. Bao, M. Jin, R. Lu, P. Xue, Q. Zhang, D. Wang, Y. Zhao, J. Solid State Chem., Vol. 175, (2003), p. 322.
 36. A. M. Qin, Y.P. Fang, W.X. Zhao, H.Q. Liu, C.Y. Su, J. Cryst. Growth, Vol. 283, (2005), p. 230.
 37. N. Gao, F. Guo, Mater. Lett., Vol. 60, (2006), p. 3697.
 38. F. H. Zhao, Q. Su, N.S. Xu, C.R. Ding, M.M. Wu, J. Mater. Sci., Vol. 41, (2006), p. 1449.
 39. W. Qingqing, Z. Gaoling, H. Gaorong, Mater. Lett., Vol. 59, (2005), p. 2625.
 40. Y. D. Li, H.W. Liao, Y.T. Qian, L. Yang, G.E. Zhou, Chem. Mater., Vol. 10, (1998), p. 2301.
 41. C. Cheng, G. Xu, H. Zhang, H. Wang, J. Cao, H. Ji, Mater. Chem. Phys., Vol. 97, (2006), p. 448.
 42. X. Guo-Yue, W. Han, C. Chuan-Wei, Z. Hai-Qian, C. Jie-Ming, J. Guangbin, Trans. Nonferrous Met. Soc. China, Vol. 16, (2006), p. 105.
 43. C. J. Barrelet, Y. Wu, D.C. Bell, C.M. Lieber, J. Am. Chem. Soc., Vol. 125, (2003), p. 11498.
 44. M. Chen, L. Pan, J. Cao, H. Ji, G. Ji, X. Ma, Y. Zheng, Mater. Lett., Vol. 60, (2006), p. 3842.
 45. L. Wang, L. Chen, T. Luo, Y. Qian, Mater. Lett., Vol. 60, (2006), 3627.
 46. X. Liu, Mater. Chem. Phys., Vol. 91, (2005), p. 212.
 47. R. Jenkins, R.L. Snyder, in: Chemical Analysis: Introduction to X-ray Powder Diffractometry, John Wiley and Sons Inc., New York, (1996), pp. 319–354.

